Journal of Molecular Graphics and Modelling 57 (2015) 27–35

Contents lists available at ScienceDirect

Journal of Molecular Graphics and Modelling

journal homepage: www.elsevier.com/locate/JMGM

Characterization of ICAM-1 biophore to design cytoadherence blocking peptides

A. Mehra[a,1], Gaurav Jerath[b,1], Vibin Ramakrishnan[b], Vishal Trivedi[a,*]

[a] Malaria Research Group, Department of Biotechnology, Indian Institute of Technology-Guwahati, Guwahati 781039, Assam, India
[b] Molecular Informatics & Design Laboratory, Department of Biotechnology, Indian Institute of Technology-Guwahati, Guwahati 781039, Assam, India

ARTICLE INFO

Article history:
Received 21 August 2014
Received in revised form
22 November 2014
Accepted 6 January 2015
Available online 13 January 2015

Keywords:
Endothelial cells
Cytoadherence
Peptide
Malaria
PfEMP1
Red blood cells

ABSTRACT

Peptides from natural sources are good starting material to design bioactive agents with desired therapeutic property. IB peptide derived from the ICAM-1 has been studied extensively as an agent to disrupt the non-specific binding of lymphocyte to the endothelial cells. ICAM-1: IB molecular model reveals that IB peptide binds in an extended conformation to the ICAM-1, masking LFA-1 and partially covering PfEMP-1 binding site. Considering the regioselective requirement of ICAM-1: PfEMP1 binding site, IB peptide charge and 3-D conformation are optimized through generation of combinatorial peptide library containing single, double, triple, tetra and quadra amino acid substitutions of IB peptide. Further, truncation of IB peptide followed by molecular modeling studies gave us the biophoric environment of the IB peptide required for its activity. Molecular modeling of these peptides into the binding site indicates that these complexes are fitting well into the site and making extensive interactions with the residues crucial for PfEMP-1 binding. Molecular dynamics simulations were performed for 10 ns each under four different temperatures to estimate comparative stability of ICAM1: IB peptide complexes. The designed peptide ICAM1: IBT213 has comparable stability at ambient temperature, while ICAM1: IBT1 shows a greater degree of robustness at higher temperatures. Overall, the study has given useful insights into IB peptide binding site on ICAM1 and its potential in designing novel peptides to disrupt the cytoadherence complex involving ICAM1: PfEMP1

1. Introduction

Cell to cell adhesion or contact is important for maintenance of the tissue integrity and exchange or transfer of the substance from the cell to cell transversely [1]. The immune system regulation and action is kept up by cell adhesion molecules that enhance the efficiency of specific lymphocyte-target cell interactions, receptor-dependent lymphocyte accessory cell, leukocyte-endothelial cell interactions, etc. LFA-1, CD2 and LFA-3 molecules show antigen-dependent T-lymphocyte adhesion [2]. A thin layer of endothelial cells present in blood-brain barrier controls the selective supply of molecules to brain [3,4]. In addition, the endothelial layer protects the brain from the direct exposure of cytotoxic agents or inflammatory molecules from immune cells [5,6]. Inflammation at brain site due to acute infection upregulates cell surface adhesion receptors to induce cellular adhesion. Abnormal cellular adhesion of RBCs to endothelial cells is responsible for vascular damage and obstruction during diabetes, malaria, hereditary hydrocytosis, sickle cell anemia [7–11]. ICAM-1, CD54 and CD36 have been identified as endothelial receptors for IRBCs [12–14]. Cytoadherence of parasitized erythrocytes is mediated by *Pf*EMP-1 expression on the surface of infected RBCs. Cytoadherence of ICAM-1 to surface expressed antigen on IRBCs leads to cascade of consequences that contribute in the development of cerebral malaria. IRBC-endothelial cells cytoadherence represent a promising target to attenuate or eliminate down-stream patho-physiological events.

ICAM-1 (interstitial cell adhesion molecule-1) belongs to the immunoglobulin-like superfamily, and it plays an important role in cell recognition, cell adhesion and cell aggregation [13]. ICAM-1 exists in both membrane-bound and soluble forms [15]. The molecule is composed of five extracellular domains that are structurally similar to immunoglobulin-like fold with glycosylation in second, third and fourth domain. Each immunoglobulin domain is composed of seven antiparallel β strands ABCDEFG. The two facing β sheets, one sheet from A, B, E and D and other by G, C and F strand gives sandwich pattern with an intramolecular disulphide bonds between B and F [16,17]. The contact site for

* Corresponding author. Tel.: +91 361 2582217; fax: +91 361 258 2249.
E-mail address: vtrivedi@iitg.ernet.in (V. Trivedi).
[1] Equal Contribution

http://dx.doi.org/10.1016/j.jmgm.2015.01.004
1093-3263/

LFA-1 Mac-1, HRV-1 and *Pf*EMP-1 molecules is located in domain 1 [18]. The adhesion site for infected RBC is predicted to be present between strands A and B [19]. The adhesion sites on ICAM-1 for *Pf*EMP-1 expressing infected RBCs are distinct from binding sites for LFA-1 and HRVs [18,19]. The residues 15-18, 20–22, 36–38 and 40–49 have been found crucial for IRBCs binding [18]. IB peptide is a 21 amino acid long peptide (amino acid sequence, QTSVSPSKVILPRGGSVLVTG), derived from the ICAM-1 has been found to inhibit the interaction between endothelial cells and T lymphocytes [20]. The designed peptide efficiently masks the LFA-1 interacting site and give relives in non-specific cytoadherence and inflammation [21]. In the current study, we have put efforts to generate amino acid substitution in the IB peptide to design a molecule to mask ICAM-PfEMP1 interaction site. Considering the regioselective requirement of ICAM-1: PfEMP1 binding site, IB peptide charge and 3-D conformation are optimized through generation of combinatorial peptide library containing single, double, triple, tetra and quadra amino acid substitutions of IB peptide. Further, truncation of IB peptide followed by molecular modeling studies could predict the activity core of the IB peptide required for its activity. Molecular modeling of these peptides into the binding site indicates that these complexes are fitting well into the site and making extensive interactions with the residues crucial for PfEMP-1 binding. Molecular dynamics simulations under four different temperatures have been performed to estimate comparative stability of ICAM1: IB peptide complexes. Overall, the study has given insights into IB peptide binding site on ICAM1 and its utility in designing novel peptides to disrupt the cytoadherence complex involving ICAM1: PfEMP1.

2. Materials and methods

2.1. Generation of inhibitory peptide library

IB peptide (QTSVSPSKVILPRGGSVLVTG) represents the starting peptide sequence to design a combinatorial peptide library consisting of 733 peptides representing single, double, triple, quadra and penta substituted peptides (Table S1). IB peptide is a part of ICAM-1 (PDB ID: 1D3L) and served as a template for molecular modeling of different peptide sequences present in peptide library[17]. 3-D structure modeling of the peptide sequence from the library was done by modeller 9v9 with the help of EasyModeller 2.0 [22]. The structural quality of each modeled peptide was checked by Procheck v3.5 [23] and Ramachandran plot [24] and most of the peptide models comply basic geometrical parameters.

2.2. Molecular modeling of peptides from the peptide library into PfEMP-1 binding site

The individual peptide from the combinatorial peptide library was fitted into the ICAM-1 3-D structure using patchdock [25]. 'FireDock' program is used initially to perform energy minimization of best 20 models to get stable ICAM1-peptide complexes [26]. Atomic contact energy (ACE) and local proximity to the predicted Pf binding sites in an ICAM-1 3-D structure was analyzed.

2.3. Determination of antigen index of peptides

Antigenicity of individual amino acid in the peptide sequence was predicted by JaMBW, a java based molecular biologist workbench (http://www.bioinformatics.org/JaMBW/3/1/7/). JaMBW utilizes the algorithm of hopp and woods [27] to computes and plot the antigenicity along the polypeptide chain.

2.4. Molecular dynamics simulations

Molecular dynamics (MD) simulations and analysis were performed in Intel Xeon Workstations using GROMACS program suite 4.6.2 [28] with GROMOS96 43A1 force field [29]. The dynamics of ICAM-1-peptide inhibitor complex were studied at four different temperatures, 300 K, 325 K, 350 K and 375 K under NVT conditions with periodic boundary. Both complexes were energy minimized in vacuum and water using steepest descent algorithm for a maximum of 2000 steps before production run. Solvent molecules (SPC water) were then added to a periodic cubic box with edges of 7.3 nm on all sides. Throughout the simulations, bond lengths were constrained using LINCS algorithm with an integration time step of 2fs. Berendsen thermostat has been employed to keep the temperature constant. Initial velocities were taken from a Maxwellian distribution at the chosen temperature bath with a coupling relaxation time of 0.1 ps. Van der Waals and electrostatic interactions were treated with a cutoff of 0.8 nm; particle mesh Ewald handled the electrostatics with a grid spacing of 0.12 nm and relative tolerance at the cutoff was set at 10^{-5}. Various programs in GROMACS package and in-house generated programs and scripts were used for conformational analysis.

3. Results

3.1. ICAM-1 has a well-defined binding site for IB peptide

IB peptide is derived from ICAM-1 and found to inhibit ICAM-1/LFA-1 mediated heterotypic T-cell cytoadherence to the epithelial cells [20]. Molecular modeling studies indicate that IB derived cyclic peptides bind to the I-domain of LFA-1 at the metal ion-dependent adhesion site [21]. ICAM-1 has a well-defined region to provide docking site for LFA-1, HRV and PfEMP-1 on domain-I to facilitate binding of T-lymphocyte, virus particle and infected RBCs (Fig. 1A). ICAM-1: IB molecular model reveals that IB binds in an extended conformation to the ICAM-1, masking LFA-1 and partially covering PfEMP-1 binding site (Figure 1B). The IB peptide has a mixed environment, a positively charged amino-terminus (-NH_2) followed by negative or neutral stretch of amino acids (2–7), weakly positive stretch (8–11), neutral amino acids (12–20) and negatively (partial) charged carboxyl end. Positively and negatively charged patches on ICAM-1 domain-I facilitate the strong binding and fitting of IB peptides to the LFA-1 and PfEMP-1 (partially) binding region (Fig. 1B). IB peptide amino acid residues interact extensively with the ICAM-1 residues by hydrogen bonding, van der Waal, hydrophobic and salt bridge (Fig. 2). T2 is in hydrogen bonding to Asp26; V4 is interacting to Tyr 66, hydrophobic interaction between V9 and Leu43, salt bridge between R13 and Lys40, as well as few weak interactions of peptide residues with domain-I residues exists (Table 1).

3.2. IB peptide can be modulated to block PfEMP-1 binding site

Peptide binding to the receptor is controlled by distribution of charges and surface area available for interaction [30]. PfEMP-1 binding site on domain-I has a characteristic charge distribution with positive, negative and hydrophobic patches (Fig. 1B). In addition, few pockets or grooves gives a 3-D topological constrains and can be exploited to design specific peptides to disrupt ICAM1:PfEMP1 cytoadherence complex. A close analysis of ICAM-1: IB molecular model indicates that IB peptide can be mutated at multiple positions to facilitate conformational changes in peptide to accommodate into the available grooves and charged patches in PfEMP-1 binding site. Keeping the information of ICAM: 1-PfEMP1 complex, hot spot residues, a rational design approach is used to

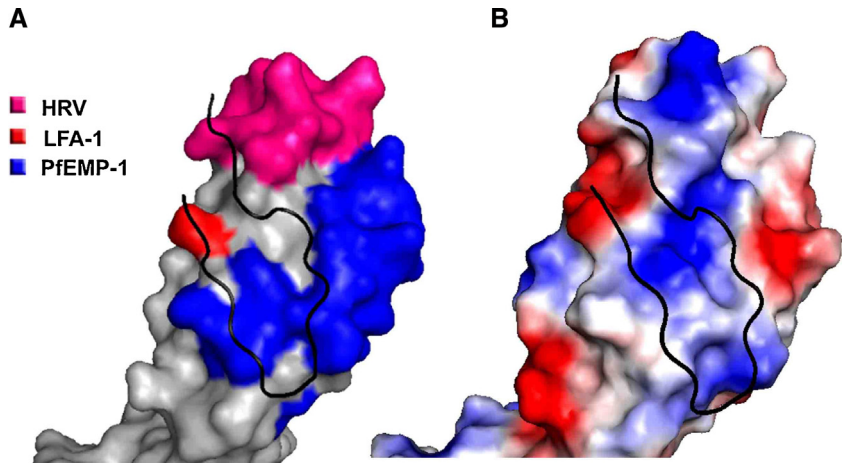

Fig. 1. ICAM-1 has well-defined region to binds IB peptide. (A) Regiospecific selectivity of ICAM for different ligands. Different regions of ICAM-1 responsible for binding LFA-1, HRV or PfEMP-1 ligand were shown with different colors; LFA-1 (orange), HRV (hot pink) and PfEMP-1 (deep blue). (B) Surface Structure of the ICAM-1 binding site for different ligands and binding mode of IB peptide. IB peptide (black) binds to the ICAM-1 in an extended conformation occupying LFA-1 and PfEMP-1 binding site. Blue is positive, red is negative colored and IB peptide (black) is displayed as in ribbon model. Figure was prepared by pymolv0.99. (For interpretation of the references to color in this figure legend, the reader is referred to the web version of this article).

design has been employed to design peptide library to optimize IB peptide to disrupt ICAM-1: PfEMP-1 cytoadherence complex (Table S1). The single, double, triple, tetra/quadra substituted peptides fit nicely to domain-I than wild-type IB peptide (Table 2). Amino acid substitution in IB peptide and resulting ICAM-1: peptide molecular models reveals a different binding mode of mutated IB peptides (Table 3). Single substitution at K8 with a hydrophobic amino acid isoleucine has multiple effects; changes the charge distribution of wild-type IB peptide (due to inductive effects of lysine), it disrupt several existing interactions of wild-type IB peptide with domain-I and lastly it allows the formation of new interaction. As a result of these multifaced changes, wild-type peptide change its binding mode on domain-I and covers a larger area of ICAM-1: PfEMP-1 cytoadherence area. Other single substitution such as T20P, S3G and S5A also made significant changes in the wild type IB binding mode and cover PfEMP-1 site (Fig. 3A). In a similar fashion binding mode of double substituted, triple substituted peptides span throughout the PfEMP-1 binding site (Fig. 3B, C). Triple substituted IB304 peptide (Q1H/S3M/T20P) binds to PfEMP-1 with a specificity but the masking region is very small (stretches of amino acids 15–18, 20–22). Most of the earlier mutation in IB peptide gives peptide that are still partially masking LFA-1 binding except Quadra substituted IB 327 peptide (S3M/V9K/L18M/T20V) (Fig. 3D). Quadra substituted peptide is masking major region (stretches of amino acids 36–38, 40–49) of PfEMP-1 binding site with a better fitting (ACE value: −486.67) to the charged surface and hydrophobic groove. IB327 exhibits several strong interactions with the residues of domain-I (Table 3); most of the interactions are much stronger (in the range of 2–4 Å) than interaction exhibited by IB peptides.

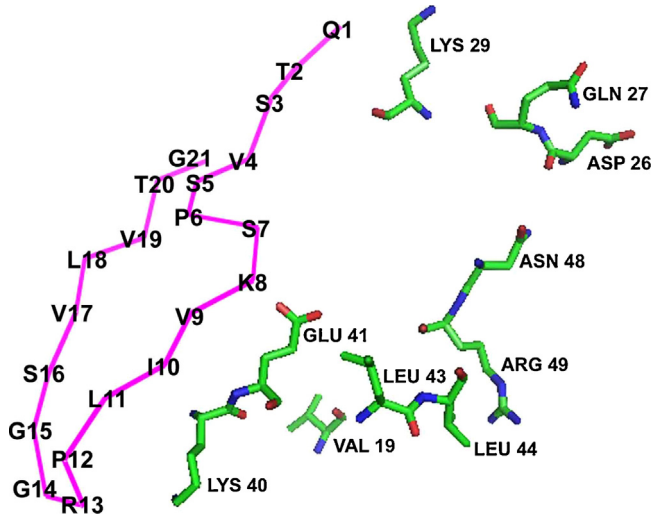

Fig. 2. Interaction of IB peptide with key residues present within the binding pocket of ICAM-1. IB peptide is making hydrogen bonding, salt bridge and other molecular interactions with the residues of ICAM-1. IB peptide residues are represented in single letter notation whereas ICAM1 residues are given in three letter notation. A details interaction with distance parameters was given in Table 1. Figure was prepared by pymolv0.99.

3.3. IB 327 peptide is immunogenic, needs truncation and optimization

Peptides are immunogenic and restrict their usage as therapeutics molecules [31,32]. Antigenic potentials of IB and IB327 peptide is evaluated as described in the method section. IB is moderately

Table 1
Interaction of IB peptide with ICAM-1 molecule.

S. no.	Peptide residue	ICAM residue	Distance (Å)
1	T2	ASP 26	4.08
2	V4	TYR66	3.5
3	S5	ASN47	3.25
4	S7	TYR66	3.30
5	K8	LEU43	4.0
6	V9	LEU43	4.33
7	V9	LEU44	4.26
8	I10	LEU43	5.52
9	L11	GLU41	3.53
10	R13	LYS40	3.02
11	G14	GLU41	4.44
12	G15	GLU41	6.43
13	S16	GLU41	8
14	V17	GLU41	5.91
15	L18**	VAL19	6.44
16	V19	LYS29	4.83
17	T20$	ARG49	5.96
18	G21	GLN27	3.07

The interactions that were found to be more than 4 Å were exercised for amino acid substitutions (such as denoted by ** and $). IB peptide residues are represented in single letter notation whereas ICAM1 residues are given in three letter notation. The interaction analysis helped in differentiating out the residues that can be substituted without causing any effect on other relevant residues.

Table 2
Summary of IB peptide optimization.

Type of variants	Peptide code	Amino acid sequence	ACE value
Wild type	Wild type	QTSVSPSKVILPRGGSVLVTG	−105.23
Single substitution	IB28	QTSVSPSIVILPRGGSVLVTG	−480.04
	IB60	QTSVSPSKVILPRGGVLVPG	−471.92
	IB16	QTGVSPSKVILPRGGSVLVTG	−460.58
	IB2	QTSVAPSKVILPRGGSVLVTG	−436.4
Double substitution	IB110	QTGVIPSKVILPRGGSVLVTG	−539.7
	IB136	QTMVPSKVIAPRGGSVLVTG	-320.17
	IB151	QTSVAPSKVILPRGGSVLVPG	−278.86
	IB141	QTMVSPSKVILPRGGSVLVVG	−262.04
Triple substitution	IB304	HTMVSPSKVILPRGGSVLVPG	−414.4
	IB296	HTSVIPSKVILPRGGSVIVTG	−402.7
	IB236	HTSVSPSKVIAPRGGSVIVTG	−389.8
	IB298	HTMVSPSKVIAPRGGSVLVTG	−506.4
Quadra substitution	IB327	QTMVSPSKKILPRGGSVMVVG	−486.67
Truncated products			
Truncation	IB 331	MVSPSKKILPRGGSVMVVG	−122.74
	IB 332	VSPSKKILPRGGSVMVVG	−212.17
	IB 333	SPSKKILPRGGSVMVVG	−37.26
	IB 334	PSKKILPRGGSVMVVG	−272.00
	IB 335	KKILPRGGSVMVVG	−105.30
	IB 336	ILPRGGSVMVVG	−329.13
	IB 337	PRGGSVMVVG	−111.34
	IB 338	GGSVMVVG	−287.41
	IB 339	GSVMVVG	−297.32
	IBT1	GSVLVT	−110.2
Single substitution	IBT13	GSVLVS	−277.56
	IBT26	GSVIVT	−240.43
	IBT24	GSVQVT	−230.1
	IBT5	GSVLVV	−229.49
Double substitution	IBT82	GSYLVA	−305.96
	IBT50	GSVIVS	−290.77
	IBT71	GSELVV	−268.31
	IBT97	GSVIHT	−266.06
Triple substitution	IBT153	GSYQLT	−246.21
	IBT151	GSYRVV	−197.72
	IBT213	GSYIVA	−178.35

immunogenic whereas S3M/V9K/L18M/T20V is potent immunogenic to generate antibodies from B-cells (Fig. 4A). Amino acid stretch (1–15) in IB 327 peptide is highly antigenic whereas 16–21 is low antigenic (Fig. 4B). Antigenicity of a peptide molecule is determined by length, complexity and evolutionary distance from host organism [33]. Sequential truncation product of IB 327 was prepared, and their fitting into the domain-I and antigenicity is determined. A hexameric peptide IBT1 (GSVLVT) has lost immunogenicity, but it's fitting is also been compromised (Table 2). Keeping the information of domain-I interaction with IBT1, hexameric peptide IBT1 is mutated at single, double, triple or quadra positions to optimize the fitting into the PfEMp-1 binding site (Table S1). Mutated hexameric IBT peptides exhibit significant improvement in binding to the PfEMP-1 binding site, and IBT213 was found as

Table 3
Comparative interaction analysis of IB327 and Peptide IBT213 with ICAM-1.

Peptide IB 327			**Peptide IBT213**		
Peptide residue	**Protein residue**	**Distance (Å)**	**Peptide residue**	**Protein residue**	**Distance (Å)**
T2	LEU43	3.91	G1	GLN27	2.85
M3	GLU41	3.38	G1	LYS29	3.37
V4	GLU41	3.91	G1	LYS29	1.95
S5	LEU42	4.56	S2	GLN27	2.19
V7	LYS40	3.15	S2	PRO28	2.32
K8	LEU37	2.19	Y3	PRO28	3.58
K9	LYS39	1.41	Y3	ASP26	1.18
I10	LEU43	3.25	Y3	GLN27	3.27
L11	LEU30	2.16	Y3	CYS25	4.44
P12	GLU34	3.02	Y3	LYS29	4.73
R13	MET64	0.95	I4	PRO28	3.02
G14	GLU41	3.86	I4	LEU30	4.16
G15	LEU30	2.82	I4	GLY32	3.86
S16	LEU30	4.3	I4	ASN47	3.87
V17	LEU30	2.45	I4	GLY46	2.95
M18	THR20	3.48	V5	ASN47	3.82
V19	GLU41	4.02	V5	LYS50	3.19
V20	LYS50	4.56	A6	LYS50	4.29
G21	LEU43	4.47	A6	GLU41	1.85

Peptide residues are represented in single letter notation whereas ICAM1 protein residues are given in three letter notation to avoid confusion.

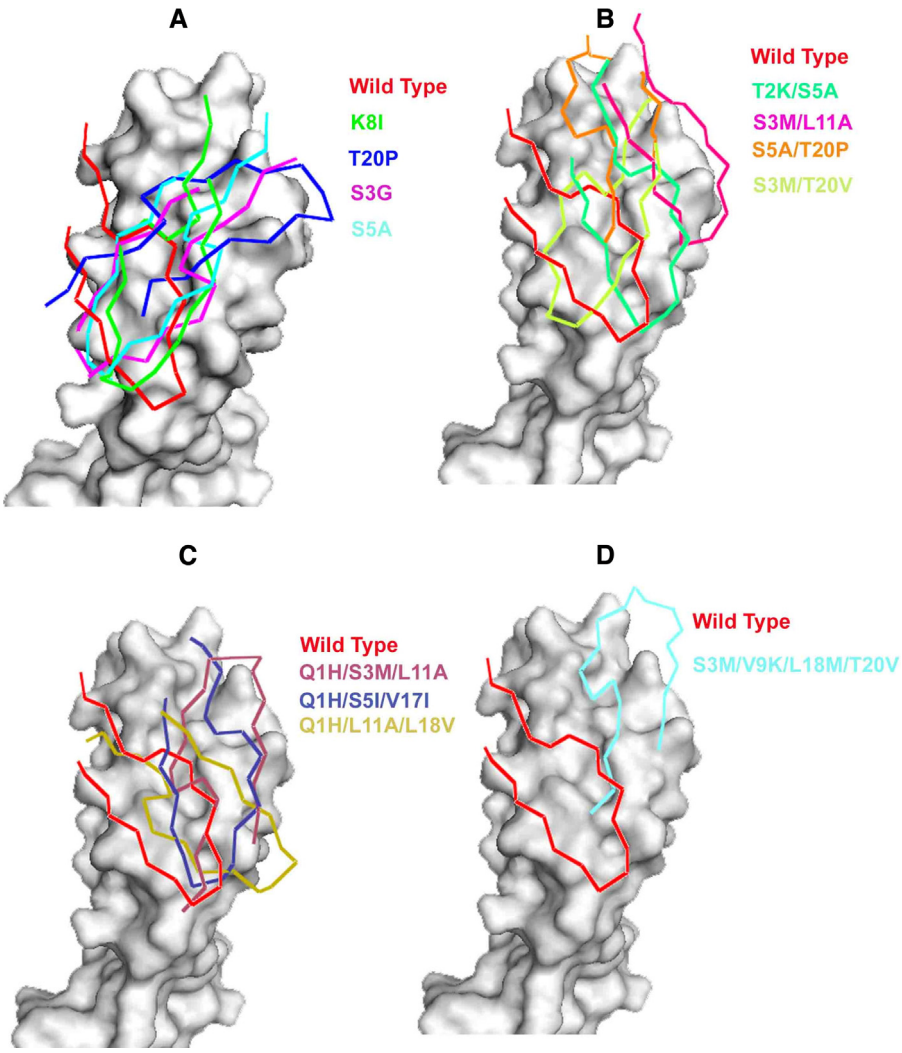

Fig. 3. Binding mode of different IB substituted peptides in ICAM-1 structure. (A) Single substitution (B) Double substitution (C) Triple Substitution and (D) Quadra substituted best IB peptide and triple substituted truncated hexapeptide. Single substituted peptides in panel A; K8I in green, T20P in blue, S3G in magenta and S5A is in cyan colored. Double substituted peptides in panel B; T2K/S5A in lime green, S3M/L11A in hot pink, S5A/T20P in orange, S3M/T20V is in lemon colored. Triple substituted peptides in panel C; Q1H/S3M/L11A in raspberry, Q1H/S5I/V17I in the deep blue, Q1H/L11A/L18V in is in olive colored. Quadra substituted best peptide is shown in aqua marine, triple substituted truncated hexapeptide is in magenta in panel D. ICAM surface, and wild-type unsubstituted IB peptide is shown in white and red respectively. Figure was prepared by pymolv0.99. (For interpretation of the references to color in this figure legend, the reader is referred to the web version of this article).

best hexameric peptide (Table 2). IBT213 fits into the stretches of amino acids 36–38, 40–49 regions of PfEMP-1 binding site (Fig. 3D).

3.4. Comparative stability analysis of peptide complexes

Molecular dynamics simulations were performed at varied temperatures as a method to both qualitatively compare binding affinity of two peptides IBT1 (GSVLVT) and IBT 213 (GSYIVA) on their designated ICAM-1 binding site and quantitatively compare the conformational stability of the complex. Simulations were performed at four different temperatures of 300 K, 325 K, 350 K and 375 K for 10 ns. Four programs g_rms, g_hbond, g_cluster and g_dist in GROMACS have been used for analysis of generated structures during production run. The root mean square deviation (RMSD) for atoms at the peptide-protein receptor site was monitored using the g_rms program. RMSD from the starting structure was found to be in the range of 0.2–0.3 nm for the ICAM1-IBT1 complex and 0.3–0.4 nm for the complex at 300 K (Fig. S1). The hydrogen binding interaction between the receptor and the peptides was mapped using the g_hbond program. The ICAM1-IBT1 showed more consistency in maintaining hydrogen bonding interactions compared to the ICAM1-IBT213 during the course of 10 ns simulation (Fig. 5). However, ICAM1-IBT213 complex could hold binding interactions at 300, 325 and 350 K. To check this, we further examined the weighted average distances of the peptide from the residues of the binding pocket with the help of g_dist program. The distance distribution as a function of time for both complexes is shown in Fig. 6, and it is evident that both the peptides are in a comparable distance range from the binding site throughout the simulation run at 300 K, 325 K and 350 K. However, it may also be noted that at 375 K, ICAM1-IBT213 complex disintegrates considerably.

The trajectory frames from the production run were clustered using the g_cluster program and the LigPlots for the clustered structures was generated using the LigPlus software package [34]. The LigPlots for both IBT1 and IBT213 peptides for the simulation at 300 K are given in the Fig. 7, the plots for the simulations at subsequent temperatures are included in Supplementary information

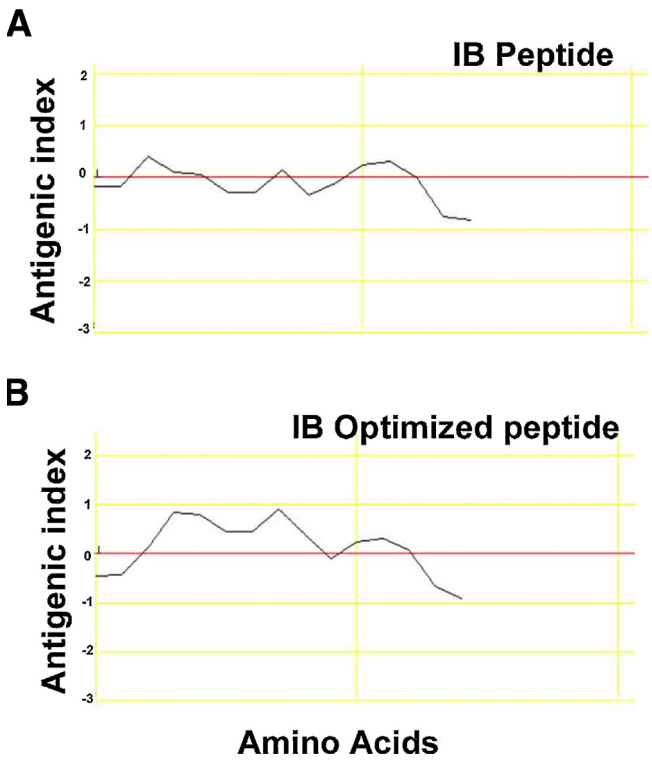

Fig. 4. Immunogenic nature of different peptide fragments. (A) Antigenic potential of IB peptide and (B) optimized IB peptide. Antigenicity of individual amino acid in the peptide sequence was predicted by JaMBW, and plot the antigenicity along the polypeptide chain.

(Fig. S2). Both the peptides seem to behave comparably under the tested conditions. However, the hydrogen bonding interaction network of the ICAM1-IBT1 complex is comparatively more robust than the ICAM1-IBT213. Simulation results hence confirm the stability of interactions for both the peptide complexes, through a simulation time that is sufficient enough to create an ensemble of structures for meaningful comparison between two protein complexes.

4. Discussion

Animal cells are involved in biological activities such as the destruction, communication to neighboring cells, generating an immune response against invading pathogens and allergic reactions. Cellular system utilizes multiple mechanisms to elicit responses under these conditions. One of the mechanisms involve the production and secretion of small peptides (6–10 amino acids) with the desired biological activity from secreting cell. In addition, target cells perceived the signal through cell surface receptor against the peptide ligand. Hence, several bioactive peptides were isolated from different sources and tested for their therapeutic applications [35]. Considering physicochemical properties as criterion, synthetic peptides were designed with desired biological activities [36]. There are two popular approaches to modulate the property of a given peptide sequence, with desirable features to suffice the needs. In the random approach, a large number of random amino acid substitutions at each residue position has been generated [37]. In an alternate approach, an intelligent guessing (based on interaction or adopting 3-D conformation) can be used to generate specific mutation in the peptide sequence to get a peptide with desired features [38].

ICAM-1 molecules expressed on endothelial cell surface have target adhesion sites for various antigenic molecules such as LFA-1, HRVs, PfEMP-1, MAC-1, MUC-1 [20,21,39,40]. There have been a large number of peptides of different sequences developed to mask the target area on ICAM-1 required for interaction, or the active sites on antigenic ligand molecule. Hence, the peptide development is started by the sequence chosen either from ICAM-1 or other antigenic molecules. Binding of fluorescently labeled Molt-4 cells to TNF stimulated human umbilical vein endothelial cells have been found to be inhibited by peptides ICAM-1 (1–20), ICAM-1 (28–50), ICAM-1 (40–64), ICAM-1 (122–146) and ICAM-1 (345–375) [20]. Three overlapping sequences of the peptides of ICAM-$1_{40–64}$ (KELLLPGNNRKVYELSNVQEDSQPM) were synthesized and tested, and the sequence KELLLPGNNRKV has shown the maximum potency. The ICAM-1 (1–21) peptide has been studied by fragmenting its sequence into overlapping cyclic peptides: cIBL. ($ICAM_{1–10}$), cIBC ($ICAM_{6–15}$), and cIBR ($ICAM_{12–21}$) [21]. These cyclic peptides were found to have higher activities than the parent peptide ($ICAM_{1–21}$) in inhibiting homotypic T-cell adhesion, MLR, and heterotypic T-cell adhesion [21]. These results suggest that the conformational restriction in cyclic peptides creates a more rigid structure that accommodates better binding to LFA-1 and blocks ICAM-1/LFA-1 interaction. The peptides from ICAM-1 origin have also been developed that are efficient in inhibiting the cytoadherence of parasitized RBC to the ECs [19]. Hexapeptide GSVLVT has inhibited the IRBC binding to endothelial cells with IC_{50} of 0.125 mM [19].

Our study has identified the potential site of interaction of IB peptide on ICAM-1 and matched well with the earlier mutation studies in ICAM-1. Based on the topology of the interaction surface and the IB peptide interactions with ICAM-1, we have generated 733 peptides with mutation (based on rational design) in IB peptide. The analysis of the ICAM-1: peptide models enabled to identify the active region of the IB peptide and allowed us to truncate the IB peptide to a hexameric sequence. It has reduced the immunogenic nature of IB peptide as well as it may enhance better bioavailability of the peptide (Fig. 4).

The stability of truncated hexameric peptide IBT1 and the optimized peptide IBT213 has been tested with the help of MD simulation. MD simulations were performed for 10 ns each, thus generating fairly large ensemble of structures under NVT conditions. Conformational analysis was principally aimed at making a comparative estimate of relative stability of two complexes ICAM1-IBT1 and ICAM1-IBT213. Root mean square deviation from the starting structure is within acceptable ranges of structural integrity, especially at lower temperatures. To examine the binding affinity, we calculated the distance between ligand and receptor binding site. Both ICAM1-IBT1 and ICAM1-IBT213 attaches to the binding site quite remarkably at 300 K, 325 K and 350 K, but with decreasing stability. AT 375 K, ICAM1-IBT213 almost completely disintegrates, showing complete detachment from the binding site. Hydrogen bonding interaction statistics further NIL this observation. Hydrogen bonding between receptor and ligand donor-acceptor pairs retain well at 300 K, while progressively decline at higher temperatures. This observation also supports the accuracy of GORMOS forcefield and 43A1 parameter sets employed for making comparative estimates of thermodynamic parameters involved protein-ligand binding interactions.

In the current study, we have utilized a combination of both approaches, initially, we have generated a random mutation in the IB peptide sequence and then performed filtration using interaction of IB peptide with ICAM-1 as a criterion (Table S1). In addition, such a filtration is performed by making single mutation, a double mutation and other mutation. Further truncation and optimization led us to the design of IBT213 as new peptide to specifically block ICAM-1: PfEMP1 interaction surface. Previous studies with GSVLVT (IBT1 in this study) shows high activity in blocking EC-RBC cytoadherence in a flow experiment. IBT 213 has approximately two fold better

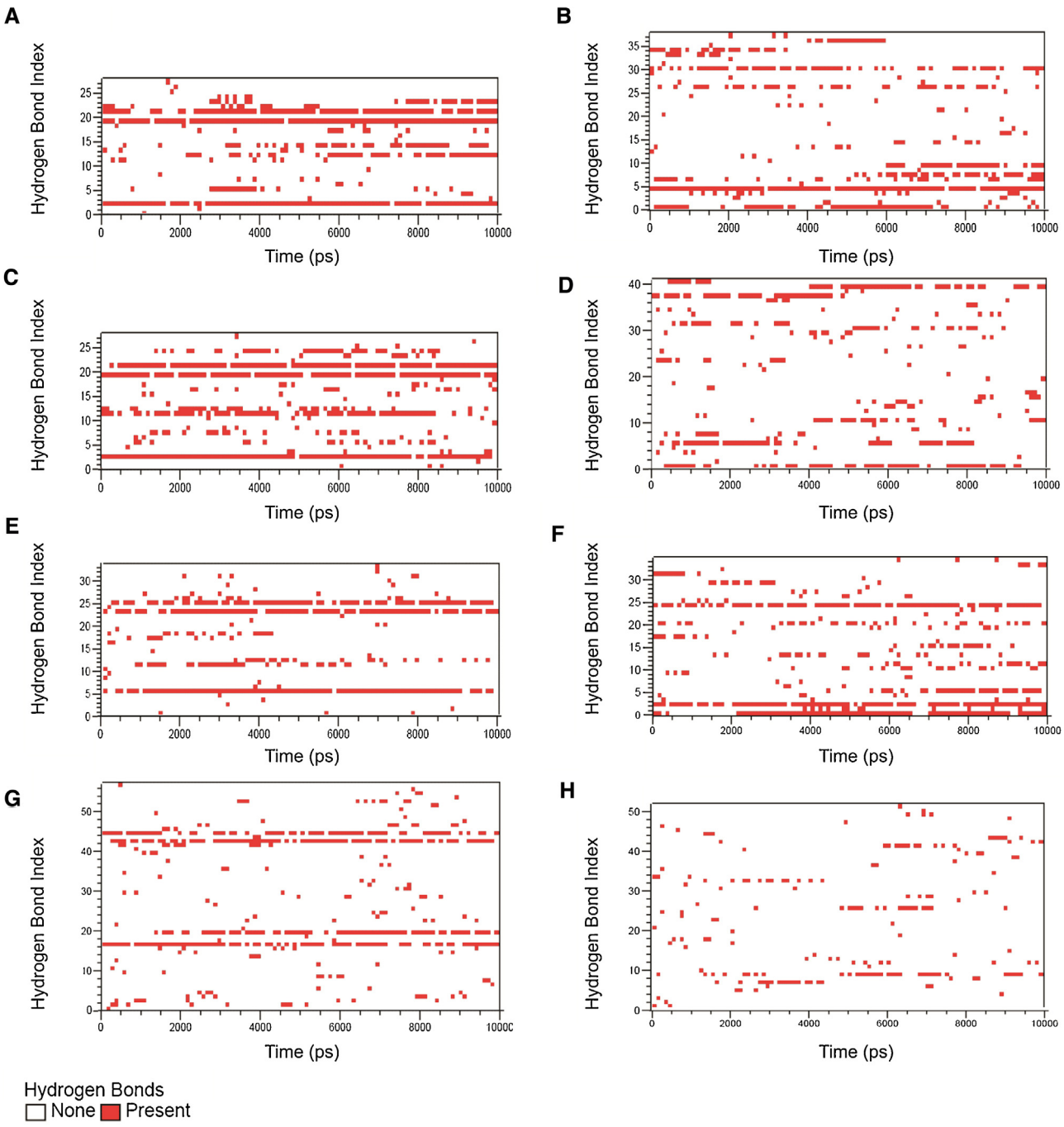

Fig. 5. Hydrogen bonding patterns of ICAM1: peptide complexes during the course of simulations. The hydrogen bonding pattern for the IBT1 (GSVLVT) and the IBT213 (GSYIVA) with the binding site on the ICAM1 at different temperatures, (A, B) 300 K, (C, D) 325 K, (E, F) 350 K and (G, H) 375 K respectively. Figure was prepared using the g_hbond command from the GROMACS package.

affinity and fitting into the ICAM-1 interaction site. Comparative MD analysis indicate that it may be equally potent in inhibiting EC-RBC cytoadherence. A supplementary study to test the inhibitory potential of IBT213 in an in-vitro cytoadherence assay may give useful information and will provide a conclusion to the current study. The purpose of the current study is to understand the forces operating between EC (ICAM-1) and RBC (PfEMP1) cytoadherence complex and designing better cytoadherence peptides. Adherence blocking peptide designed in the study may be useful for development of potential anti-adhesion therapeutics.

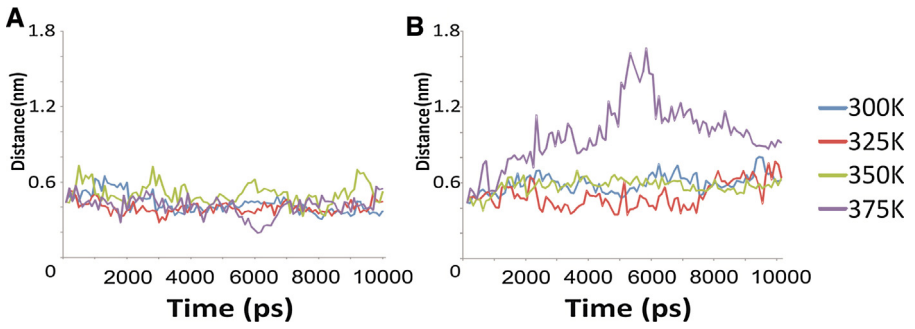

Fig. 6. Distance of Peptides from the ICAM1: PfEMP1 Binding site. The distance of the IBT1 (GSVLVT) (A) and IBT213 (GSYIVA) (B) from the binding pocket as a function of time during the M.D. simulation. Figure was prepared using the g_dist command from the GROMACS package.

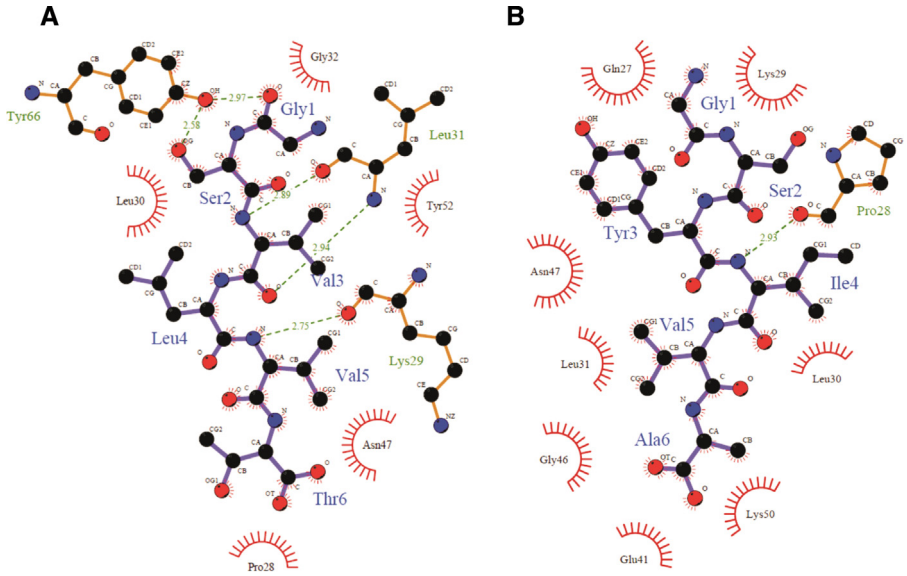

Fig. 7. LigPlots for the peptides after a 10 ns M.D. simulation at 300 K temperature. The LigPlots for the ICAM1: peptide complexes were generated for the largest clusters (A) IBT1 (GSVLVT) (B) IBT213 (GSYIVA). The amino acid residue names in blue denote the peptides, while all the other residues denote the binding site residues of the ICAM 1. Figure was prepared using the g_cluster command from GROMACS package and the LigPlus tool. (For interpretation of the references to color in this figure legend, the reader is referred to the web version of this article).

Acknowledgment

This work was supported by the Department of Biotechnology; Govt of India Grants (102/IFD/SAN/2628–2643/2013–2014) to V.T.

Appendix A. Supplementary data

Supplementary data associated with this article can be found, in the online version, at http://dx.doi.org/10.1016/j.jmgm.2015.01.004.

References

[1] S.A. Desai, Why do malaria parasites increase host erythrocyte permeability? Trends Parasitol. 30 (3) (2014) 151–159.
[2] T.A. Springer, et al., The lymphocyte function-associated LFA-1, CD2, and LFA-3 molecules: cell adhesion receptors of the immune system, Annu. Rev. Immunol. 5 (1987) 223–252.
[3] G.S. Hillis, A.D. Flapan, Cell adhesion molecules in cardiovascular disease: a clinical perspective, Heart 79 (5) (1998) 429–431.
[4] D. Faille, et al., Platelet microparticles: a new player in malaria parasite cytoadherence to human brain endothelium, FASEB J. 23 (10) (2009) 3449–3458.
[5] T. Stevens, et al., Mechanisms regulating endothelial cell barrier function, Am. J. Physiol. Lung Cell Mol. Physiol. 279 (3) (2000) L419–L422.
[6] H. Lum, A.B. Malik, Mechanisms of increased endothelial permeability, Can. J Physiol. Pharmacol. 74 (7) (1996) 787–800.
[7] F. Marques, et al., Blood-brain-barriers in aging and in Alzheimer's disease, Mol. Neurodegener. 8 (2013) 38.
[8] N. Reymond, B.B. d'Agua, A.J. Ridley, Crossing the endothelial barrier during metastasis, Nat. Rev. Cancer 13 (12) (2013) 858–870.
[9] M.H. Wang, K.S. Kim, Cytotoxic necrotizing factor 1 contributes to *Escherichia coli* meningitis, Toxins (Basel) 5 (11) (2013) 2270–2280.
[10] M. Canavese, R. Spaccapelo, Protective or pathogenic effects of vascular endothelial growth factor (VEGF) as potential biomarker in cerebral malaria, Pathog. Glob. Health 108 (2) (2014) 67–75.
[11] J.L. Wautier, M.P. Wautier, Molecular basis of erythrocyte adhesion to endothelial cells in diseases, Clin. Hemorheol. Microcirc. 53 (1–2) (2013) 11–21.
[12] G. Turner, Cerebral malaria, Brain Pathol. 7 (1) (1997) 569–582.
[13] A.G. Craig, A.R. Berendt, The role of ICAM-1 as a receptor for rhinovirus and malaria, Chem. Immunol. 50 (1991) 116–134.
[14] J.D. Chulay, C.F. Ockenhouse, Host receptors for malaria-infected erythrocytes, Am. J. Trop. Med. Hyg. 43 (2 Pt 2) (1990) 6–14.
[15] S. Hashimoto, et al., Elevated levels of soluble ICAM-1 in sera from patients with bronchial asthma, Allergy 48 (5) (1993) 370–372.
[16] P.R. Kolatkar, et al., Structural studies of two rhinovirus serotypes complexed with fragments of their cellular receptor, EMBO J. 18 (22) (1999) 6249–6259.
[17] J. Bella, et al., The structure of the two amino-terminal domains of human ICAM-1 suggests how it functions as a rhinovirus receptor and as an LFA-1 integrin ligand, Proc. Natl. Acad. Sci. U S A 95 (8) (1998) 4140–4145.
[18] A.R. Berendt, et al., The binding site on ICAM-1 for Plasmodium falciparum-infected erythrocytes overlaps: but is distinct from, the LFA-1-binding site, Cell 68 (1) (1992) 71–81.
[19] C.F. Ockenhouse, et al., Plasmodium falciparum-infected erythrocytes bind ICAM-1 at a site distinct from LFA-1: Mac-1, and human rhinovirus, Cell 68 (1) (1992) 63–69.
[20] S.A. Tibbetts, et al., Peptides derived from ICAM-1 and LFA-1 modulate T cell adhesion and immune function in a mixed lymphocyte culture, Transplantation 68 (5) (1999) 685–692.
[21] S.A. Tibbetts, et al., Linear and cyclic LFA-1 and ICAM-1 peptides inhibit T cell adhesion and function, Peptides 21 (8) (2000) 1161–1167.

[22] B.K. Kuntal, P. Aparoy, P. Reddanna, EasyModeller a graphical interface to MODELLER, BMC Res. Notes 3 (2010) 226.
[23] R.A. Laskowski, D.S. Moss, J.M. Thornton, Main-chain bond lengths and bond angles in protein structures, J. Mol. Biol. 231 (4) (1993) 1049–1067.
[24] G.N. Ramachandran, C. Ramakrishnan, V. Sasisekharan, Stereochemistry of polypeptide chain configurations, J. Mol. Biol. 7 (1963) 95–99.
[25] D. Schneidman-Duhovny, et al., PatchDock and SymmDock: servers for rigid and symmetric docking, Nucleic Acids Res. 33 (2005) W363–W367 (Web Server issue).
[26] N. Andrusier, R. Nussinov, H.J. Wolfson, FireDock: fast interaction refinement in molecular docking, Proteins 69 (1) (2007) 139–159.
[27] L.H. Holley, M. Karplus, Protein secondary structure prediction with a neural network, Proc. Natl. Acad. Sci. U S A 86 (1) (1989) 152–156.
[28] S. Pronk, et al., GROMACS 4.5: a high-throughput and highly parallel open source molecular simulation toolkit, Bioinformatics 29 (7) (2013) 845–854.
[29] W.R.P. Scott, et al., The GROMOS biomolecular simulation program package, J. Phys. Chem. 103 (2013) 3596–3607.
[30] J.N. Ma, et al., Discovery of novel peptide/receptor interactions: identification of PHM-27 as a potent agonist of the human calcitonin receptor, Biochem. Pharmacol. 67 (7) (2004) 1279–1284.
[31] C.M. Smith, et al., Novel immunogenic peptides elicit systemic anaphylaxis in mice: implications for peptide vaccines, J. Immunol. 187 (3) (2011) 1201–1206.
[32] A. Sun, J. Fang, J. Yan, Advance and development in research of bacterial drug-resistance signaling mechanism and multiple antigenic peptide-based vaccines, Zhejiang Da Xue Xue Bao Yi Xue Ban 42 (2) (2013) 125–130.
[33] H.J. Dyson, P.E. Wright, Antigenic peptides, FASEB J. 9 (1) (1995) 37–42.
[34] A.C. Wallace, R.A. Laskowski, J.M. Thornton, LIGPLOT: a program to generate schematic diagrams of protein-ligand interactions, Protein Eng. 8 (2) (1995) 127–134.
[35] F. Shahidi, Y. Zhong, Bioactive peptides, J. AOAC Int. 91 (4) (2008) 914–931.
[36] D.D. Kitts, K. Weiler, Bioactive proteins and peptides from food sources Applications of bioprocesses used in isolation and recovery, Curr. Pharm. Des. 9 (16) (2003) 1309–1323.
[37] A. Shrivastava, A.D. Nunn, M.F. Tweedle, Designer peptides: learning from nature, Curr. Pharm. Des. 15 (6) (2009) 675–681.
[38] P. Zhou, et al., Computational peptidology: a new and promising approach to therapeutic peptide design, Curr. Med. Chem. 20 (15) (2013) 1985–1996.
[39] J.L. Kam, et al., MUC1 synthetic peptide inhibition of intercellular adhesion molecule-1 and MUC1 binding requires six tandem repeats, Cancer Res. 58 (23) (1998) 5577–5581.
[40] D.I. Baruch, et al., CD36 peptides that block cytoadherence define the CD36 binding region for *Plasmodium falciparum*-infected erythrocytes, Blood 94 (6) (1999) 2121–2127.